International Journal of Science and Research (IJSR)
ISSN (Online): 2319-7064
Index Copernicus Value (2013): 6.14 | Impact Factor (2013): 4.438

Formability of Warm Deep Drawing Process for AA1050-H18 Pyramidal Cups

A. Chennakesava Reddy

Professor, Department of Mechanical Engineering, JNT University, Hyderabad-500 085, India

Abstract: ***In this present work, a statistical approach based on Taguchi Techniques and finite element analysis were adopted to determine the formability of pyramidal cup using warm deep drawing process. The process parameters were thickness of blank, temperature, coefficient of friction and strain rate. The experimental results were validated using a finite element software namely D-FORM. The AA1050 –H18 sheets were used for the deep drawing of the pyramidal cups. The blank thickness by itself has a substantial effect on the effective stress and the height of the pyramidal cup drawn. The reduction of the drawing force was perceived with the increase of temperature. The effective stress increases with the increase of friction due to increase of normal pressure between die and blank. The formability of the pyramidal cups was outstanding for the surface expansion ratio greater than 2.9. The strain hardening exponent values for 0.8, 1.0 and 1.2 mm thick blank sheets have been found to be 0.28, 0.30 and 0.33 respectively. The formability of deep drawn pyramidal cups is difficult with blank thickness less than 1mm.***

Keywords: AA1050-H18, warm deep drawing, thickness, temperature, coefficient of friction, strain rate, pyramidal cups, formability.

1. Introduction

The deep drawing process is a forming process which occurs under a combination of tensile and compressive conditions. When drawing complex products in practice, there is usually a combination of stretch and deep drawing involved. Common deep drawn products are cans, boxes, and bottles, as well as irregularly shaped products. Parts produced by hot forming are characterized by high strength, complex shapes.

The formability limitations of conventional deep drawing are a barrier for some industrial uses. Radial drawing stress and tangential compressive stress are a common concern that can result in wrinkling, fracturing or cracking in some applications. The process variables, which affect the failure of the cup drawing process, include material properties, die design, and process parameters such as temperature, coefficient of friction, strain rate, blank holding force, punch and die corner radii and drawing ratio. The ductility of common aluminum alloys increases with temperature. Thus forming at elevated temperatures close to the recrystallization temperature of about 300 °C, also called warm forming, is one of the promising methods to improve formability. The deep drawing process of an aluminum alloy has been simulated to study the deformation behavior and the temperature change and successfully predicted the forming limit and necking site by comparing the numerical results with experimental results [1]. In a research on low carbon steel, the results conclude that with enhancement of strain rate and reduction of temperature, the tensile strength increases and entire flow curve of material increases its level [2]. Friction is another important parameter that influences the deep drawing process. In metal forming processes, the friction influences the strain distribution at tool blank interface and drawability of metal sheet. In the experimental work carried out on the warm deep drawing process of the EDD steel it has been observed that the extent of thinning at punch corner radius is found to be lesser in the warm deep-cup drawing process of extra-deep drawing (EDD) steel at 200^0C [3]. In another work performed by the author [4] on the cup drawing process using an implicit finite element analysis, the thinning is observed on the vertical walls of the cup with high values of strain at the thinner sections. In the finite element simulations, a forming limit diagram (FLD) has been successfully applied to analyze the fracture phenomena by comparing the strain status [5].

AA1050 is known for its excellent corrosion resistance, high ductility and highly reflective finish. Applications of AA1050 are typically used for chemical process plant equipment, food industry containers, architectural flashings, lamp reflectors, and cable sheathing. AA1050 aluminum alloy is not heat treatable. It is difficult to deep draw and to have minimum wall thickness of less than 1 mm. Therefore, it is expensive to exploit the combination of high strength and thin wall cups using deep drawing process.

In the present work, the formability of warm deep drawing process was assessed during the fabrication of AA1050-H18 pyramidal cups. The investigation was focused on the process parameters such as blank thickness, temperature, coefficient of friction and strain rate. The design of experiments was carried out using Taguchi technique and the warm deep drawing process was executed using the finite element analysis software namely D-FORM 3D.

Table 1: Control parameters and levels

Factor	Symbol	Level–1	Level–2	Level–3
Thickness, mm	A	0.8	1.0	1.2
Temperature, ^{0}C	B	300	400	500
Coefficient of friction	C	0.05	0.075	0.1
Strain rate, 1/s	D	1	5	10

2. Materials and Methods

AA1050-H18 was used to fabricate pyramidal cups. The levels chosen for the control parameters were in the operational range of AA1050-H18 aluminum alloy using deep drawing process. Each of the three control parameters was studied at three levels. The chosen control parameters are summarized in table 1. The orthogonal array (OA), L9 was selected for the present work. The parameters were assigned

to the various columns of O.A. The assignment of parameters along with the OA matrix is given in table 2.

Table 2: Orthogonal array (L9) and control parameters

Treat No.	A	B	C	D
1	1	1	1	1
2	1	2	2	2
3	1	3	3	3
4	2	1	2	3
5	2	2	3	1
6	2	3	1	2
7	3	1	3	2
8	3	2	1	3
9	3	3	2	1

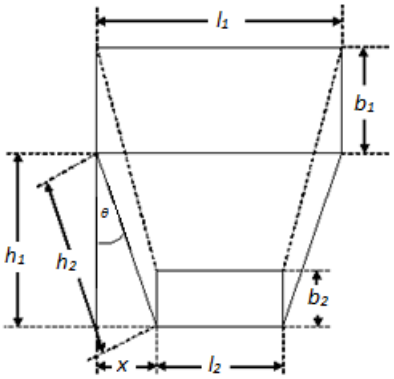

Figure 1: Initial dimensions (without corner & edge radii) of the pyramidal cup

The initial dimensions of the pyramidal cup without corner and edge radii are shown in figure 1. The blank size is calculated by equating the surface area of the finished drawn cup with the area of the blank. The blank dimensions are obtained by:

$$(l_1 + l_2 + b_1 + b_2)h_2 + l_2 b_2 = l_b b_b \quad (1)$$

where l_1 and l_2 are the top and bottom lengths of the pyramidal cup respectively; $h_1$and h_2 are the height and slant heights of cup respectively; b_1 and b_2 are top and bottom widths of the cup respectively.

In the present work, the dimensions of the cup are as follows:

Cup top length, l_1 = 60 mm
Cup top width, b_1 = 40 mm
Slant angle, θ = 6 degrees
Height of the cup, h_1 =75 mm

The slant height, h_2 of the pyramidal cup is given by the following expression:

$$h_2 = \frac{h_1}{cos\theta} \quad (2)$$

The bottom length, l_2 of the pyramidal cup is given by the following expression:

$$l_2 = l_1 - 2x \quad (3)$$

The bottom width, b_2 of the pyramidal cup is given by the following expression:

$$b_2 = b_1 - 2x \quad (4)$$

where, $x = h_2 \times sin\,\theta$

In order to avoid wrinkling in the pyramidal cup, the blank must be given corner radius, r_c which can be expressed as follows:

$$r_c = \sqrt{{r_{cp}}^2 + 2r_{cp}h_1 - 1.41 r_{cp} r_{ep}} \quad (5)$$

where, r_{cp} is the punch side corner radius and r_{ep} is the punch edge radius.

The top and bottom dimensions of the punch are equal to the top and bottom dimensions of the cup. The height of the punch is the height of the cup. The drawing punch must have corner radius exceeding one-tenth of the cup top length. The radius joining the bottom to the sides, r_{ep} generally ranges from three to eight times the blank thickness (t). In the present work, the corner and edge punch radii are taken as below:

$$r_{cp} = l_1/5 \text{ and } r_{ep} = 5t \quad (6)$$

The material flow in drawing may render some flange thickening and thinning of walls of the cup inevitable. The space for drawing is kept bigger than the sheet thickness. This space is called die clearance.

$$\text{Clearance, } c_d = t \pm \mu\sqrt{10t} \quad (7)$$

where μ is the coefficient of friction.

The top length of the die is obtained from the following equation:

$$l_{d1} = l_1 + 2c_d \quad (8)$$

The bottom length of the die is obtained from the following equation:

$$l_{d2} = l_2 + 2c_d \quad (9)$$

The top width of the die is obtained from the following equation:

$$b_{d1} = b_1 + 2c_d \quad (10)$$

The bottom width of the die is obtained from the following equation:

$$b_{d2} = b_2 + 2c_d \quad (11)$$

The height of the die is the height of the cup. The corner radius of the die is obtained by the addition of clearance to the punch corner radius. The edge radius of the die is eight times the blank thickness.

3. Finite Element Modeling and Analysis

The finite element modeling and analysis was carried using D-FORM 3D software. The pyramidal sheet blank was created with desired diameter and thickness using CAD tools [6]. The pyramidal top punch, pyramidal bottom hollow die were also modeled with appropriate inner and outer radius and corner radius using CAD tools. The clearance between the punch and die was calculated as in Eq. (9). The sheet blank was meshed with tetrahedral elements [7]. The modeling parameters of deep drawing process were as follows:

Number of tetrahedron elements for the blank: 21980
Number of nodes for the blank: 7460
Number of polygons for top die: 9120
Number of polygons for bottom die: 9600

The basic equations of the rigid-plastic finite element analysis are as follows:

Equilibrium equation:

$$\sigma_{ij,j} = 0 \quad (12)$$

Compatibility and incompressibility equations:

$$\text{Strain rate tensor, } \dot{\varepsilon}_{ij} = \frac{1}{2}\left(u_{i,j} + u_{j,i}\right), \dot{\varepsilon}_{kk} = 0 \quad (13)$$

where $u_{i,j}$ and $u_{j,i}$ are velocity vectors.

Constitutive equations:

$$\text{Stress tensor, } \sigma_{ij} = \frac{2\sigma_{eq}}{3\varepsilon_{eq}}\dot{\varepsilon}_{ij} \quad (14)$$

where, equivalent stress, $\sigma_{eq} = \sqrt{\frac{3}{2}\left(\sigma'_{ij}, \sigma'_{ij}\right)}$ and equivalent strain, $\varepsilon_{eq} = \sqrt{\frac{3}{2}\left(\dot{\varepsilon'_{ij}}\dot{\varepsilon'_{ij}}\right)}$.

The Coulomb's friction model was given by

$$\tau_f = \mu p \quad (15)$$

where μ is the coefficient of friction (COF), p is the normal pressure, and τ_f is the frictional shear stress.

The flow stress based on the strain hardening is computed by the following equation:

$$\sigma_f = K\varepsilon^n \quad (16)$$

where, K and n are work hardening parameters depending on mechanical properties of material.

The flow stress equation considering the effects of the strain, strain rate and temperature is given by

$$\sigma_f = f\left(\varepsilon, \dot{\varepsilon}, T\right) \quad (17)$$

where, ε represents the strain, $\dot{\varepsilon}$ represents the strain rate and T represents the temperature.

Johnson-Cook Model [8] is among the most widely used mode. It connects all the deformation parameters in the following compact form.

$$\sigma_f = [\sigma + K\varepsilon^n]\left[1 + Sln\frac{\dot{\varepsilon}}{\dot{\varepsilon_0}}\right]\left[1 - \left(\frac{T-T_0}{T_m-T_0}\right)^m\right] \quad (18)$$

where, $\dot{\varepsilon_0}$ is a reference strain rate taken for normalization; σ is the yield stress and K is the strain hardening factor, whereas S is a dimensionless strain rate hardening coefficient. Parameters n and m are the power exponents of the effective strain and strain rate.

Hill's and Swift's theories used to calculate the forming limit strains on the left and the right side, respectively, of the forming limit diagram (FLD). Assuming that the strain-stress relationship of sheets can be expressed by Hollomon's equation the formulae calculating the forming limit strains can be written as follows, with stress ratio, $\alpha = \sigma_1/\sigma_2$.

For $\varepsilon_2 < 0$

$$\varepsilon_{l1} = \frac{1+(1-\alpha)r}{1+\alpha}n \quad (19)$$

$$\varepsilon_{l2} = \frac{\alpha+(1-\alpha)r}{1+\alpha}n \quad (20)$$

Normal anisotropy value represents the ratio of the natural width deformation in relation to the thickness deformation of a strip specimen elongated by uniaxial tensile stress:

$$r = \frac{\varepsilon_w}{\varepsilon_t} \quad (21)$$

For $\varepsilon_2 > 0$

$$\varepsilon_{l1} = \frac{(1+r_0-r_0\alpha)\left[1+r_0+\alpha^2\left(\frac{r_0}{r_{90}}\right)(1+r_{90})-2\alpha r_0\right]}{(1+r_0-r_0\alpha)^2+\alpha\left(\alpha\frac{r_0(1+r_{90})}{r_{90}}-r_0\right)^2}n \quad (22)$$

$$\varepsilon_{l2} = \frac{(1+r_0-r_0\alpha)\left[\alpha+\alpha r_0-\alpha^2 r_0+\alpha^2\left(\frac{r_0}{r_{90}}\right)(1+r_{90})-r_0\right]}{(1+r_0-r_0\alpha)^2+\alpha\left(\alpha\frac{r_0(1+r_{90})}{r_{90}}-r_0\right)^2}n \quad (22)$$

For plasticity studies, the basic definition of r-value has been replaced with the instantaneous r_i value, which is defined as

$$r_i = \frac{d\varepsilon_w}{d\varepsilon_t} \quad (23)$$

In the present work, the contact between blank/punch and die/blank were coupled as contact pair (figure 2). The mechanical interaction between the contact surfaces was assumed to be frictional contact and modeled as Coulomb's friction model as defined in Eq. (15). The finite element analysis was chosen to find the metal flow, effective stress, height of the cup, and damage of the cup. The finite element analysis was carried out using D-FORM 3D software according to the design of experiments.

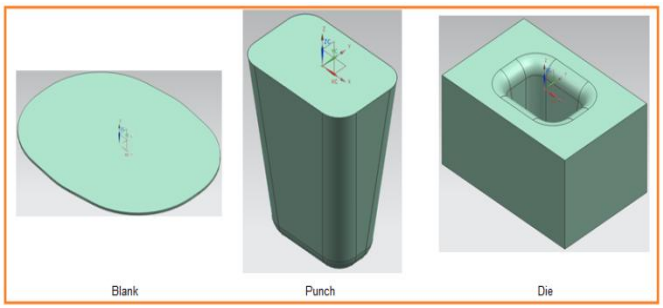

Figure 2: Deep drawing process for pyramidal cups.

4. Results and Discussion

Two trials were carried out with different meshes for each experiment. For the ANOVA (analysis of variance) the Fisher's test (F = 3.01) was carried out on all the parameters (A, B, C and D) at 90% confidence level.

4.1 Influence of process parameters on effective stress

Table 3 gives the ANOVA (analysis of variation) summary of the effective stress. The blank thickness (A) by itself had a substantial effect (68.46%) on the effective stress. The temperature had a pronounced effect of 26.20% on the effective stress. The coefficient of friction had contributed 4.51% of the total variation observed in the effective stress. The strain rate was negligible towards variation in the effective stress.

Table 3: ANOVA summary of the effective stress

Source	Sum 1	Sum 2	Sum 3	*SS*	*v*	*V*	*F*	*P*
A	400.50	669.6	785.00	12976.24	2	6488.12	102.71	68.46
B	712.10	662.8	480.20	4975.05	2	2487.52	39.38	26.20
C	567.70	669.8	617.60	868.85	2	434.42	6.88	4.51
D	607.10	616.4	631.60	50.99	2	25.49	0.40	0.20
e				63.17	9	7.02	0.11	0.63
T	2287.40	2618.6	2514.40	18934.30	17			100

Note: *SS* is the sum of square, *v* is the degrees of freedom, *V* is the variance, *F* is the Fisher's ratio, *P* is the percentage of contribution and *T* is the sum squares due to total variation.

The effective stress was increased with an increase in the blank thickness (figure 3a). In fact, the increase in the effective stress was due to the requirement of high drawing pressures for thick sheets to undergo plastic deformation. While drawing the pyramidal cups, the compressive and tensile stresses were induced along the thickness direction. These stresses would increase with an increase in the blank thickness (figure 3b). The compressive strains were predominant in the cups drawn with blank thickness of 0.8 and 1.0 mm, while the tensile strains were strongest in the cups of 1.2 mm blank thickness (figure 4). The influence of temperature on the effective stress is shown in figure 3b. The effective stress was decreased with the increase of temperature. With the

increase of temperature the cup material became soft and thereby the stress induced in the cup material would decrease due to reduction of the drawing force (figure 5). The influence of friction on the effective stress is shown in figure 3c. In this work, the coefficient of friction was varied from 0.05 to 0.1. Therefore, the shear stress due to friction would vary from 0.05P to 0.1P, where P is the normal pressure according the Eq. (15). The normal pressures developed in the pyramidal cup drawn under trials 1 and 9 are shown in figure 6. The maximum normal pressure of 2390 MPa was observed for trial 8 of the deep drawing process. The increase in the nominal contact pressure would crush the surface asperities of the blank giving rise to more real contact area. Hence, the result was the requirement of high drawing pressure to draw the pyramidal cup. The stress is defined as force/area. The denominator term would increase with an increase in thickness of the blank sheet, but this increase was dominated by the required drawing force to draw the pyramidal cups. Therefore, the effective stress was increased with the increase of friction.

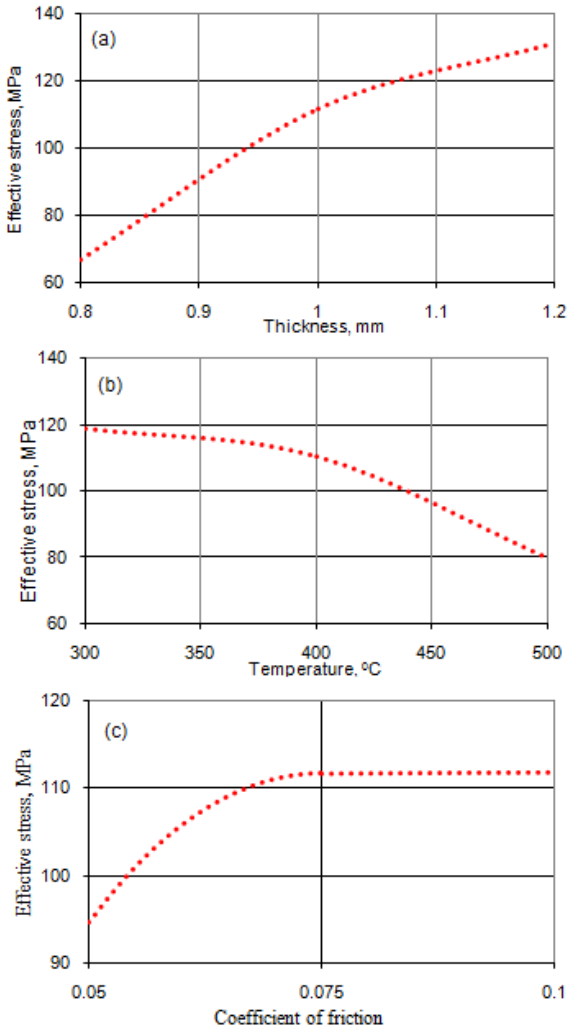

Figure 3: Influence of process parameters: (a) blank thickness, (b) temperature and (c) coefficient of friction on effective stress.

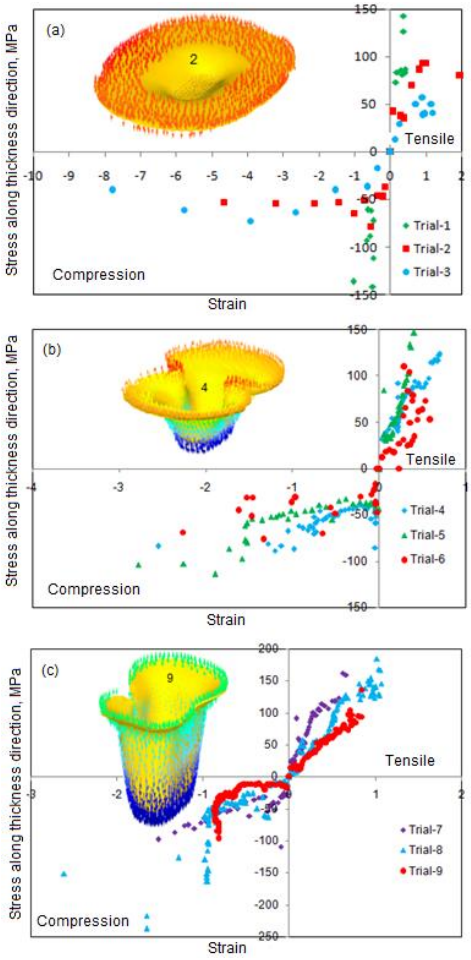

Figure 4: Stress along thickness direction (a) 0.8 mm, (b) 1.0 mm and (c) 1.2 mm blank thickness.

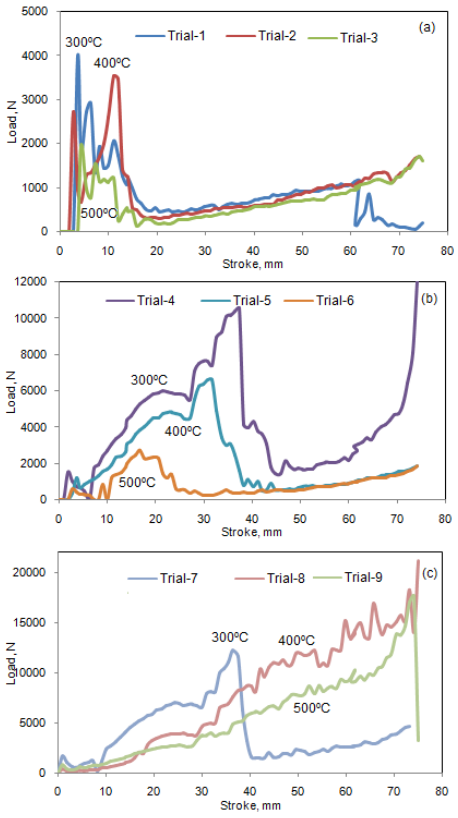

Figure 5: Influence of temperature on load (a) 0.8 mm, (b) 1.0 mm and (c) 1.2 mm blank thickness.

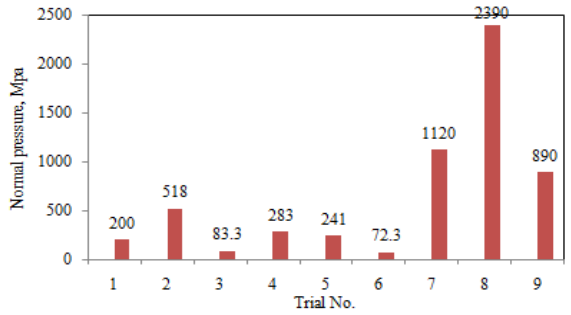

Figure 6: Influence of friction on (a) effective stress and (b) normal pressure.

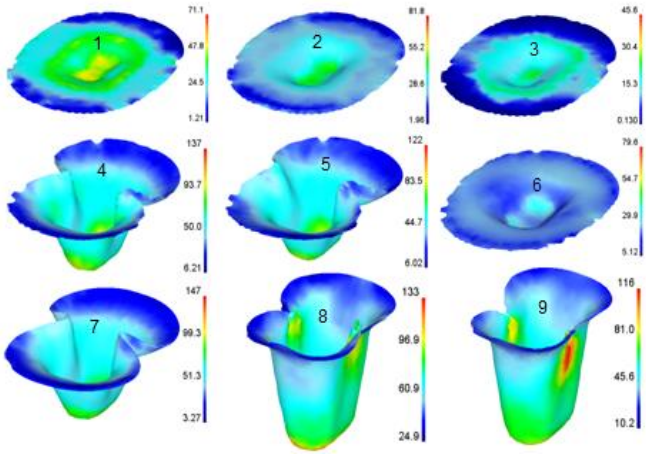

Figure 7: Effect of process parameters on the effective stress.

The FEA results of effective stress are shown in figure 7 for various test conditions as per the design of experiments. It was found that the effective stress was less than or nearly equal to the yield strength (145MPa) of the AA10550-H18 for the cups without failure.

4.2 Influence of Process Parameters on Surface Expansion Ratio

The material formability is an evaluation of how much deformation a material can undergo before failure. In the deep drawing process the plastic deformation in the surface is much more pronounced than in the thickness. The author introduces the term surface expansion ratio to measure the formability of cups. This depicts the formability and ductility of the blank material drawn into the cup.

$$\text{Surface expansion ratio} = \frac{A_i}{A_0} \qquad (24)$$

where, A_i is the instantaneous surface area of the cup drawn and A_0 is the initial blank surface area.

Table 4: ANOVA summary of the surface expansion ratio

Source	Sum 1	Sum 2	Sum 3	*SS*	*v*	*V*	*F*	*P*
A	7.66	12.72	17.36	7.85	2	3.93	34.72	71.81
B	11.27	13.25	13.22	0.43	2	0.22	1.94	3.76
C	11.87	14.92	10.95	1.43	2	0.72	6.36	12.93
D	13.84	10.52	13.38	1.08	2	0.54	4.77	9.72
e				0.11	9	0.01	0.09	1.78
T	44.64	51.41	54.91	10.90	17			100

The ANOVA summary of surface expansion ratio is given in table 4. As per the Fisher's test (F = 3.01), the blank thickness (A) all by itself would contribute the most (71.81%) towards the variation observed in the surface expansion ratio. The coefficient of friction, strain rate and temperature, respectively had contributed 12.93%, 9.72% and 3.76% towards the total variation in the surface expansion ratio.

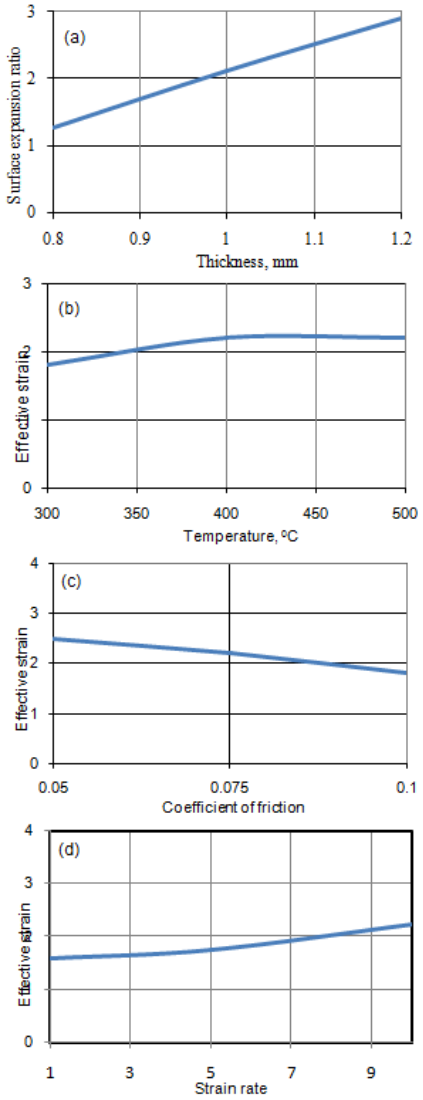

Figure 8: Influence of process parameters: (a) blank thickness, (b) temperature, (c) coefficient of friction and (d) strain rate on surface expansion ratio.

The surface expansion ratio would increase with an increase in the blank thickness (figure 8a). In the forming processes, the volume of the material remains constant before and after the forming process. On account of the punch force, the blank material undergoes plastic deformation to form the cup. As the plastic deformation is irreversible, the cup retains its shape. Experimentally, it has been observed that the surface area of the cup drawn is always higher than the initial blank surface area [4]. An increase in temperature would increase the surface expansion ratio (figure 8b). The grains get elongated on account of temperature in the direction normal to the direction of applied force, i.e. in the lateral direction. The influence of friction on the surface expansion ratio is shown in figure 8c. With the increased coefficient of friction between blank and dies, the plastic deformation was

more stable (showing fewer tendencies to folding) resulting large expansion of the blank material. The effect of strain rate on the surface expansion ratio is shown in figure 8d. The value of the stress at an arbitrary time point would only depend on the current values of strain, strain rate and temperature. A sudden change of strain rate from $\dot{\varepsilon}1$ to $\dot{\varepsilon}_2$ would lead to a corresponding increase of stress from σ_1 to σ_2. After each sudden change of $\dot{\varepsilon}$, a stress transient was observed. Depending on the previous deformation history, the stress may be at first either higher or lower than the expected value. This phenomenon represents the microstructural state and can be determined in terms of structural change during the deformation process. The present phenomenon of strain rate effect on elongation is thought to be related to the pre-existence of grain boundary micro-voids in the blank material (figure 9). The extending deformation of grain boundary micro-voids towards the tensile direction would contribute more to the total elongation, as the strain rate increases; this should be the most possible reason for the increase of surface expansion ratio with an increase in the strain-rate.

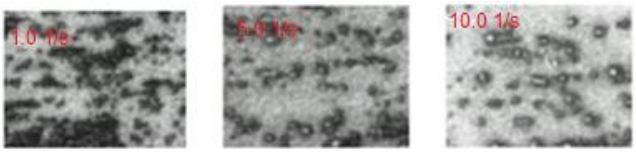

Figure 9: Micro-voids at the grain boundaries in the blank material.

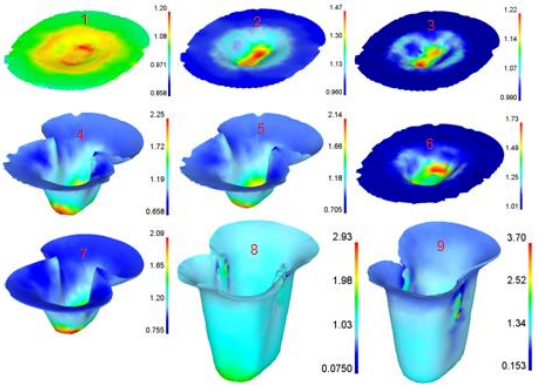

Figure 10: Effect of process parameters on the surface expansion ratio.

The FEA results of surface expansion ratio are revealed in figure 10 for various test conditions as per the design of experiments. For the surface expansion ratio greater than 2.9 the height of the cups was between 71 to 75mm. For the trails 1, 2, 3, and 6 the surface expansion ratios were lower than 2.0 yielding the cup height in the range of 7 to 16 mm. For the trails 4, 5 and 6 the surface expansion ratios were between 2.0 to 3.0 yielding the cup height in the range of 40 to 42 mm.

4.3 Influence of process parameters on cup height

As per the Fisher's test (F = 3.01), the blank thickness (A) all by itself would contribute the most (80.05%) towards the variation observed in the cup heights (table 5). The strain rate gave 11.01% towards the total variation in the cup heights. The temperature and coefficient of friction had a little influence on the height of the cup drawn.

Table 5: ANOVA summary of the effective stress

Source	Sum 1	Sum 2	Sum 3	*SS*	*v*	*V*	*F*	*P*
A	54.58	200.13	375.46	8604.98	2	4302.49	7079.96	80.05
B	180.44	251.77	197.96	460.58	2	230.29	378.95	4.28
C	190.72	254.59	184.86	498.67	2	249.33	410.28	4.64
D	245.83	141.26	243.08	1183.87	2	591.93	974.05	11.01
e				0.61	9	0.07	0.12	0.02
T	671.57	847.75	1001.36	10748.71	17			100

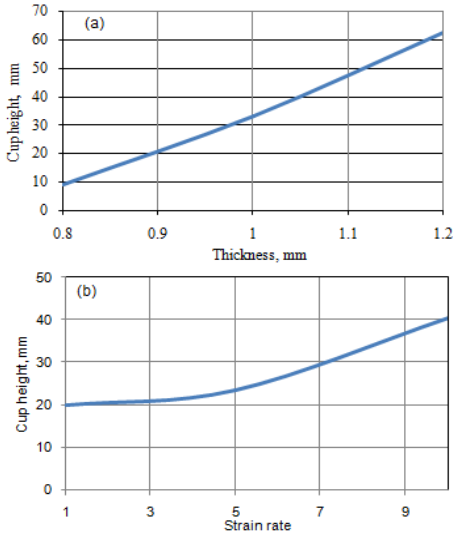

Figure 11: Influence of blank thickness (a) and strain rate (b) on the height of cup.

The cup height would increase with an increase in the blank thickness (figure 11a). This was owing to the availability of material for the plastic deformation with the increase of blank thickness. The cup height would increase with an increase in the strain rate (figure 11b). Due to increase of the friction coefficient, the normal contact pressure between the dies and blank material would also increase. The major influential characteristic of the material is the ductility which depends upon the strain rate. With the blank thickness of 0.8 mm, the maximum cup height drawn was 12.01 mm. The cup height was in the range of 16 to 42 mm for the cups drawn with the blank thickness of 1.0 mm. the cup height in the range of 42 to 74 mm was obtained with the blank thickness of 1.2 mm (figure 12). The cups which were having surface expansion ratio greater than 3.0 were drawn to the designed height (74 mm) of the pyramidal cup, as shown in figure 9.

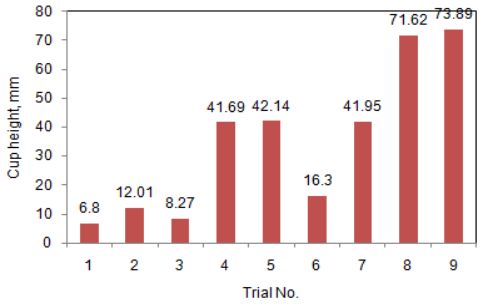

Figure 12: Cup heights under different trials

4.4 Influence of process parameters on damage of cup

The ANOVA summary of damage of cups is given in table 6. When the Fisher's test (3.01) was applied to ascertain the influence of process parameters it was found that the blank thickness (A), temperature (B), the coefficient of friction (C) and the strain rate (D), respectively had contributed 41.40%), 11.81%, 26.45% and 20.29% of the total variation in the cups heights drawn.

Table 6: ANOVA summary of damage of the cups

Source	Sum 1	Sum 2	Sum 3	*SS*	*v*	*V*	*F*	*P*
A	80.29	33.54	34.92	235.87	2	117.94	744.36	41.40
B	61.13	33.72	53.90	67.31	2	33.66	212.44	11.81
C	36.98	37.64	74.13	150.73	2	75.37	475.69	26.45
D	31.26	68.49	49.00	115.61	2	57.80	364.80	20.29
e				0.16	9	0.02	0.13	0.05
T	209.66	173.39	211.95	569.68	17			100

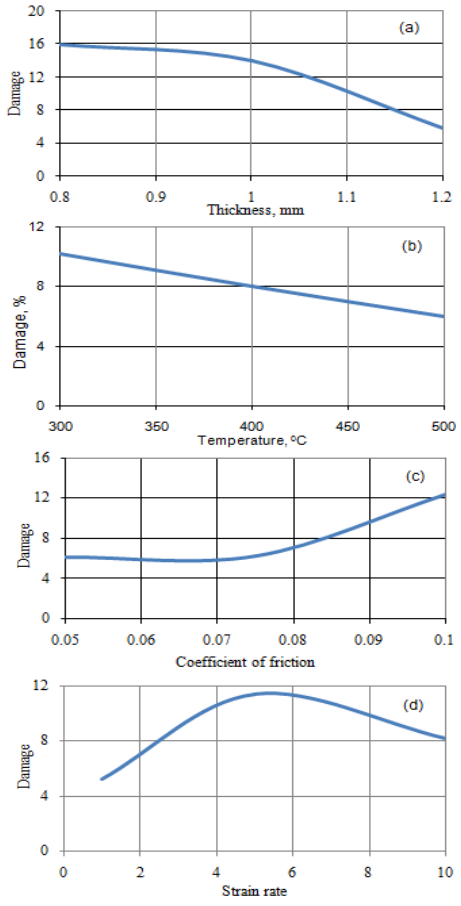

Figure 13: Influence of blank thickness on the damage of cup.

The damage factor in the cups is defined as follows:

$$D_f = \int \frac{\sigma_1}{\sigma_{es}} d\varepsilon \qquad (25)$$

where, σ_1 is the tensile maximum principal stress; σ_{es} is the effective stress; and $d\varepsilon$ is the effective strain increment.

The damage in the pyramidal cups was decreased with an increase in the blank thickness and temperature (figure 13a & 13b). The damage was increased with coefficient of friction (figure 13c). The folding of sheet was happened with the combination of low friction coefficient and thin blank sheets (0.8 & 1.0 mm), whereas there was no or less folding with the thick (1.2 mm) blank sheets and high coefficient of friction. In the case of friction between the blank and the tool, the increase of the coefficient of friction determines the wrinkling to reduce, but high values of the friction coefficient may cause cracks and material breakage [9]. The damage was found to be high with the strain rate of 5 s^{-1} (figure 13d). This is owing to the increase of yield strength with increasing of strain rate or with decreasing temperature [2]. The plastic deformation increases with the extended yield strength, consequently the damage decreases.

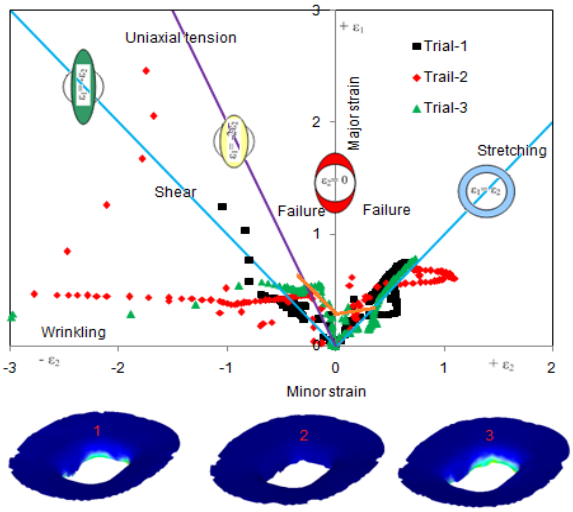

Figure 14: Forming limit diagram with damage in the cups of 0.8 mm blank thickness

Figure 14 depicts the forming limit diagram with damages in the pyramidal cups drawn from AA1050-H18 sheets of 0.8 mm. The pyramidal cups drawn under trials 1, 2 and 3 were fractured on account of shear and stretching induced in the blank material. For these cups, the minor strain was greater than the major strain. The maximum damage (18.19) was observed with trial 3. The damage in these cups is because of insufficient stretching. The blank material was cut at the corner radius of the punch. Figure 15 illustrates the forming limit diagram with damages in the pyramidal cups drawn from AA1050-H18 sheets of 1.0 mm. The pyramidal cup drawn under trials 4, 5 & 6 were fractured due to uniaxial tension and stretching. In these pyramidal cups the fracture was also observed at the punch corner radius. The pyramidal cups drawn under trial 8 were torn in the flange area owing to equal biaxial tension, whereas the cups drawn under trial 7 were fractured due to shear and stretching (figure 16). 98.37% of designed height (75 mm) of the pyramidal cups was achieved under the trial 9. The damage in the pyramidal cups drawn under trial 8 & 9 was found to be very low (figure 17). On long-side walls of the cups the stretching and

bending were witnessed; whereas the compression and bending were observed on short-side walls of the pyramidal cups. The circumferential compression was also noticed in the corners of the pyramidal cups. Overall, the compression was higher than the tension in the blank material. For most materials, forming limit curve intersects the major strain axis at the point equivalent to n-value. As n-value increases, the limit strain level increases. The n-values for 0.8, 1.0 and 1.2 mm thick blank sheets were found to be 0.28, 0.30 and 0.33 respectively. There was strain localization due to local weakness (particularly at punch corner radius) of the blank material could be observed in terms of localized necking in biaxial stretching.

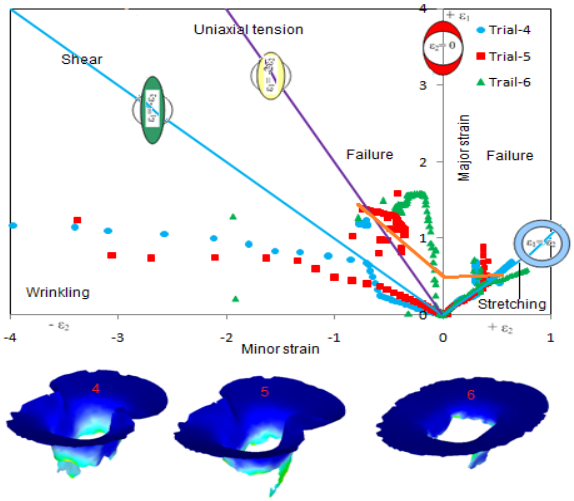

Figure 15: Forming limit diagram with damage in the cups of 1.0 mm blank thickness

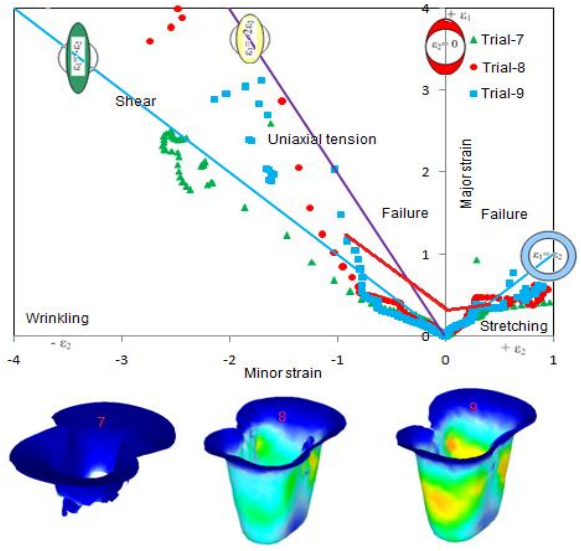

Figure 16: Forming limit diagram with damage in the cups of 1.2 mm blank thickness

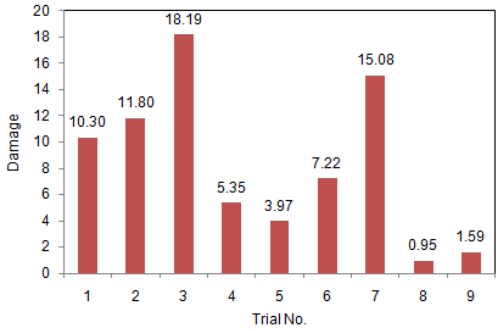

Figure 17: The damage and maximum principal strains of cups with BHF

5. Conclusions

The blank thickness by itself has a substantial effect on the effective stress and the height of the pyramidal cup drawn. With the increase of temperature the cup material becomes soft and thereby the stress induced in the cup material decreases due to reduction of the drawing force. The effective stress increases with the increase of friction due to increase of normal pressure between die and blank. For the surface expansion ratio greater than 2.9 the height of the cups is between 71 to 75mm. The damage in the pyramidal cups is decreased with an increase in the blank thickness and temperature. The pyramidal cups drawn with the blank thickness of 0.8 mm are fractured on account of shear and stretching. The pyramidal cups drawn with the blank thickness of 1.0 mm are fractured due to uniaxial tension and stretching. The damage in the pyramidal cups drawn with the blank thickness of 1.2 mm is very low. The strain hardening exponent (*n*) values for 0.8, 1.0 and 1.2 mm thick blank sheets are found to be 0.28, 0.30 and 0.33 respectively.

With further research work the forming limit diagram (FLD) will be determined with applied blank holding force to establish additional material behavior at various blank thicknesses.

6. Acknowledgment

The author wishes to thank University Grants Commission (UGC), New Delhi, India for financial assisting this project.

References

[1] H. Takuda, K. Mori, I. Masuda, Y. Abe, & M. Matsuo, “Finite element simulation of warm deep drawing of aluminum alloy sheet when accounting for heat conduction,” Journal of Materials Processing Technology, vol.120, pp.412–418, 2002

[2] K.P. Rao, Y. K. D. V. Prasad, & E. B. Hawbolt,. “Hot deformation studies on a low – carbon steel: Part I – Flow curves and the constitutive relationship,” Journal of materials processing technology, vol.56, pp.897–907, 1996.

[3] A. Chennakesava Reddy, T. Kishen Kumar Reddy, & M. Vidya Sagar, “Experimental characterization of warm deep drawing process for EDD steel,” International Journal of Multidisciplinary Research & Advances in Engineering, vol4, pp.53-62, 2012.

[4] A. Chennakesava Reddy, "Evaluation of local thinning during cup drawing of gas cylinder steel using isotropic criteria," International Journal of Engineering and Materials Sciences, vol.5, pp.71-76, 2012.
[5] F. Shehata, M. J. Painter, & R. Pearce, "Warm forming of aluminum/magnesium alloy sheet," Journal of Mechanical Working Technology, vol.2, pp.279-291, 1978.
[6] Chennakesava R Alavala, CAD/CAM: Concepts and Applications, PHI Learning Solutions Private Limited, New Delhi, 2007.
[7] Chennakesava R Alavala, Finite Element Methods: Basic Concepts and Applications, PHI Learning Solutions Private Limited, New Delhi, 2008.
[8] G. R. Johnson, & W. H. Cook, "A constitutive model and data for metals subjected to large strains, high strain rates and high temperatures. In Proceedings of the Seventh Symposium on Ballistics, The Hague, The Netherlands, pp.1-7, 1983.
[9] J. Hedworth, & M.J. Stowell, "The measurement of strain-rate sensitivity in superplastic alloys," Journal of Material Science vol.6, pp.1061–1069, 1971.